Food and Chemical Toxicology 133 (2019) 110754

Contents lists available at ScienceDirect

Food and Chemical Toxicology

journal homepage: www.elsevier.com/locate/foodchemtox

Spectrum-effect relationship of antioxidant and tyrosinase activity with *Malus pumila* flowers by UPLC-MS/MS and component knock-out method

Wenjing Li[a,b,1], Yan Zhang[c,1], Shujin Shi[d], Gen Yang[a,b], Zhenhua Liu[a,b,**], Jinmei Wang[a,b,***], Wenyi Kang[a,b,*]

[a] National R & D Center for Edible Fungus Processing Technology, Henan University, Kaifeng, 475004, China
[b] Joint International Research Laboratory of Food & Medicine Resource Function, Henan Province, Kaifeng, 475004, China
[c] Hebei Food Inspection and Research Institute, Shijiazhuang, 050091, China
[d] College of Pharmacy, Henan University of Traditional Chinese Medicine, Zhegnzhou, 450046, China

ARTICLE INFO

Keywords:
Malus pumila flower
Spectrum-effect relationship
Knock-out

ABSTRACT

The active components of *Malus pumila* flowers on antioxidant and tyrosinase activity were investigated with the method of spectrum-effect relationship and knock-out. Some compounds were identified by UPLC-MS/MS method. The chemical fingerprints were established by HPLC and the activity of antioxidant and tyrosinase were assayed *in vitro*. Chromatographic peaks P34, P35, P39, P44, P45 and P49 were identified as phloridzin, hyperoside, astragalin, afzelin, quercetin and kaempferol by UPLC-MS/MS method. Hyperoside and kaempferol were identified in *M. pumila* flowers for the first time. When the concentration was 1 g/mL of sample (equivalent to raw material), the scavenging capacity of P35 (hyperoside) on DPPH free radicals were consistent with the spectrum-effect relationship. The scavenging capacity of P34 (phloridzin) and P45 (quercetin) on ABTS free radicals were consistent with the spectrum-effect relationship. The activation effect of P45 (quercetin) on tyrosinase was consistent with the spectrum-effect relationship. The inhibitory effect of P34 (phloridzin), P35 (hyperoside) on tyrosinase were consistent with the spectrum-effect relationship.

1. Introduction

Malus pumila Mill has a long history of cultivation and is widely cultivated in temperate regions of the world (Flora of China Beijing, 1974). The main chemical constituents of *M. pumila* flowers are flavonoids (Yin et al., 2016b). In our group, nine compounds, including phloretin, kaempferol and kaempferol-7-O-β-D- glucopyranoside were isolated from *M. pumila* flowers and their anticoagulant activities were studied (Yin et al., 2018). In addition, three flavonoids in *M. pumila* flowers were analyzed by ionic liquids and exhibited activation or inhibition activity on tyrosinase (Li et al., 2018). However, the chemical compositions of *M. pumila* flowers were complex, and the dose-effect relationship between chemical compositions and activity were not completely clear.

Fingerprint spectra are a recognized method used worldwide to evaluate the quality of Traditional Chinese Medicine (TCM) (Zheng et al., 2014). The study of spectrum-effect relationship can reveal the material basis of the therapeutic values of TCM. The spectrum-effect relationship researches were conducted based on different fields, origins, harvest times, processing methods and batches of TCM (Shi et al., 2018; Cui et al., 2016; Zhao et al., 2016; Xiao, 2013, Xu, 2014). It can not only remedy the disadvantage of isolation between chemical components and pharmacodynamics, but also effectively combine fingerprint with pharmacodynamics (Cai et al., 2017).

The spectrum-effect relationship of TCM was investigated by mathematical model to connect the characteristic peaks with the pharmacodynamic value, and explore the correlation between them to provide a reliable method for elucidating the material basis of TCM (Wang et al., 2017a,b). HPLC, UPLC, GC and GC-MS are the methods to establish the fingerprints (Zhou et al., 2008). “Effective” information is obtained by the biological models *in vitro* or *in vivo* (Zhang et al., 2012).

* Corresponding author. National R & D Center for Edible Fungus Processing Technology, Henan University, Kaifeng, 475004, China.
** Corresponding author. National R & D Center for Edible Fungus Processing Technology, Henan University, Kaifeng, 475004, China.
*** Corresponding author. National R & D Center for Edible Fungus Processing Technology, Henan University, Kaifeng, 475004, China.
E-mail addresses: liuzhenhua623@163.com (Z. Liu), wangjinmeiscp@126.com (J. Wang), kangweny@hotmail.com (W. Kang).
[1] These authors contributed equally to this work.

https://doi.org/10.1016/j.fct.2019.110754
Received 8 July 2019; Received in revised form 5 August 2019; Accepted 7 August 2019
Available online 08 August 2019
0278-6915/ © 2019 Elsevier Ltd. All rights reserved.

The methods of data processing, include principal component analysis (PCA), canonical correlation analysis (CCA), partial least squares analysis (PLSR) and grey relational analysis (GRDA), are used for the most (Zhao et al., 2004).

In this study, fingerprints were established by HPLC, activity of antioxidant and tyrosinase were established for pharmacodynamic evaluation. The fingerprint peaks were correlated with pharmacodynamic data to establish a spectrum-effect model (Zeng et al., 2015). The active substances were screened by spectrum-effect relationship. The target components were isolated by component knock-out method (Xiao et al., 2009; Gong et al., 2015 and Wang et al., 2014). The activity of antioxidant and tyrosinase *in vitro* for the target components, negative samples and total extracts were evaluated.

2. Materials and methods

2.1. Chemicals and materials

Methanol was purchased from Tianjin DaMao Chemical Reagent Factory (Tianjin, China). Acetic acid was obtained from Tianjin Fuchen Chemical Reagent Factory (Tianjin, China). Astragalin with purity greater than 98% was purchased from Chengdu Pufei De Biotech Co., Ltd. (Chengdu, China). Phlorizin and afzelin with purity greater than 98% were isolated in our previous research. 1,1-diphenyl-2- picrylhydrazyl (DPPH) was obtained from Tokyo Chemical Industry Co, Ltd (Japan). Azinobis(3-ethylbenzo-thiazoline-6-sulfoncicacid) (ABTS) were obtained from Fluka (Japan). Butylatedhydroxytoluene (BHT), butyl-phydroxyanisole (BHA) and propyl gallic acid (PG) were obtained from Sigma (St. Louis, MS, USA). The LC-20AT high performance liquid chromatography system (Shimadzu, Kyoto, Japan) equipped with a degasser, a quaternary gradient low pressure pump, the CTO-20A column oven, a SPD-M20AUV-detector, an SIL-20A auto sampler was used. Chromatographic separation was performed on an Agilent ZORBAX SB-C18 column (4.6 mm × 5 mm, 5 μm) and extraction was carried out with KQ-500DB ultrasonic cleaner (Jiangsu Kunshan Ultrasonic Instrument Co., Ltd. Jiangsu, China). Electron, New York, NY, USA). The Mass spectrometer contained Q-Exactive four stage rod-orbit trap LC-MS/MS system purchased from Thermo Fisher Scientific (Waltham, MA, USA) and Thermo Ultimate 3000 UHPLC system.

2.2. Plant materials

The flowers of *M. pumila* were collected in April 2018 in Henan University (Kaifeng, Henan, China) and identified by Professor Changqin Li of National R & D Center of Edible Fungus Processing Technology. They were collected fifteen different trees. Specimens were deposited in the National Center R & D of Edible Fungus Processing Technology.

2.3. Extraction methods

The 15 batches of *M. pumila* flowers were extracted with 70% ethanol by maceration for three times, 48, 48 and 24 h, respectively. Finally, the filtrates were dried, and then methanol solution was added. The concentration was equivalent to the amount of raw material at the concentration of 1 g/mL (diluted the concentration in a test).

2.4. HPLC analysis

Chromatographic conditions: RP-18 endcapped column (4.6 mm × 250 mm, 5 μm), mobile phase with methanol-0.1% phosphoric acid water was used. The elution procedure was shown in Table 1. The flow rate was 0.8 mL/min, the column temperature was 30 °C, the UA detection wavelength was 254 nm, and the injection volume was 10 μL.

Table 1
The time program of gradient elution.

Time	methanol	0.1% phosphoric acid
0–30min	5%~24%	95%~76%
30–75min	24%~44%	76%~56%
75–90min	44%~46%	56%~54%
90–120min	46%~60%	54%~40%

2.5. Determination of biological activity

2.5.1. DPPH assay

According to the literature with BHA, BHT and PG as positive control (Kang et al., 2011), the IC_{50} value of the samples was calculated by Origin 8.0 software.

Free radical scavenging rate = $(1\text{-}OD_1/OD_{2)} \times 100\%$

2.5.2. ABTS assay

According to the literature with BHA, BHT and PG as positive control (Kang et al., 2010), the scavenging rate of ABTS free radicals and IC_{50} value were calculated.

2.5.3. Activity of tyrosinase assay

According to the reference (Zhang et al., 2014), the ethanol extracts were prepared into corresponding concentration to determine the activity of tyrosinase. The activation rate of tyrosinase was calculated according to the formula.

$$\textit{Tyro}\ \text{sin}\ \textit{ase activation rate} = \left[\frac{A(\text{sample+substrate+enzyme}) - A(\text{sample + substrate})}{A(\text{DMSO+substrate+enzyme}) - A(\text{DMSO + substrate})} - 1 \times 100\%\right]$$

2.6. Partial least squares analysis

"Chinese traditional medicine chromatographic fingerprint similarity evaluation system 2004, 1.0 A Edition" was used to correct the retention time of each peak. The peak area was processed by equalization to obtain the quantitative data (Wang et al., 2017a,b). The partial least squares regression equation was established with the analysis software DPS 7.05. The peak area was set as the independent variable (X). Biological activation rate was taken as the dependent variable (Y). Chromatographic peaks, which were significantly correlated with activation effects on biological activation were determined, respectively.

2.7. Knock-out method

M. pumila flowers were prepared at 1 g/mL (equivalent to raw material) with 20 μL of injection volume every time under the optimized chromatography conditions. The eluent solution of the target components and negative solution without the target components were collected according to the peak retention time from the spectrum-effect relationship analysis, respectively. Each component was prepared and

eluted in a 15-fold series. The filtrated solution contained the target component (denoted as P+) and the corresponding negative sample (denoted as P-).

2.8. UPLC-MS/MS conditions

Chromatographic column was Waters BEHC 18 column (2.1 nm × 100 nm, 1.7 μm) with flow rate as 10 UL/min. Mobile phase was 0.1% formic acid-water (A) and acetonitrile (B) with gradient elution mode as 0–5 min: 10% B; 5–30 min: 10–95% B; 30–55 min: 95% B; 55–56 min. 95%–10% B, 56–61 min: 10% B. Flow rate was 0.3 mL/min. The injection volume was 0.2 UL and the column temperature was 25 °C.

Mass Spectrometric Conditions: Positive and negative modes were adopted by UPLC-MS/MS. Ionization mode was electrospray ionization (ESI) with flow rate at 35 arb. Auxiliary gas flow rate was 10 arb with spray voltage at3.5 kV. Capillary temperature was 320 degrees centigrade with scanning range for 100–1500 *m/z*, resolution 70000. Automatic Gain Control (AGC) was 3×10^6, maximum injection time was 50 ms. The isolation window was set to 4.0 *m/z*.

3. Results and discussions

3.1. Spectrum-effect relationships

3.1.1. Quantitative determination of chromatographic peaks

The flow chart of this study was shown in Fig. 1. In this study, fingerprint spectra were used to circumvent the weaknesses of the fingerprint technique and foster the strengths in TCM and to investigate spectrum-effect relationships of TCM (Xu et al., 2014). "Traditional Chinese Medicine chromatographic fingerprint similarity evaluation system (2004, 1.0A Edition)" was used to quantitatively determine the chromatographic peaks. Multi-point correction of chromatographic peak position was performed based on chromatographic peaks, which were found in each sample with good separation by reference to the chromatogram of *M. pumila* flowers. A contrast chromatogram was generated by the average method. The results showed that 49 common peaks were matched by 15 characteristic maps in Fig. 2 and Table 2.

3.1.2. Cluster analysis

The relative peak area of each common peak was taken as an index. SPSS 19.0 software was used for cluster analysis by correlation coefficient as distance measure of sample similarity (Liu et al., 2016). The results were shown in Fig. 3 and 15 batches of *M. pumila* flowers

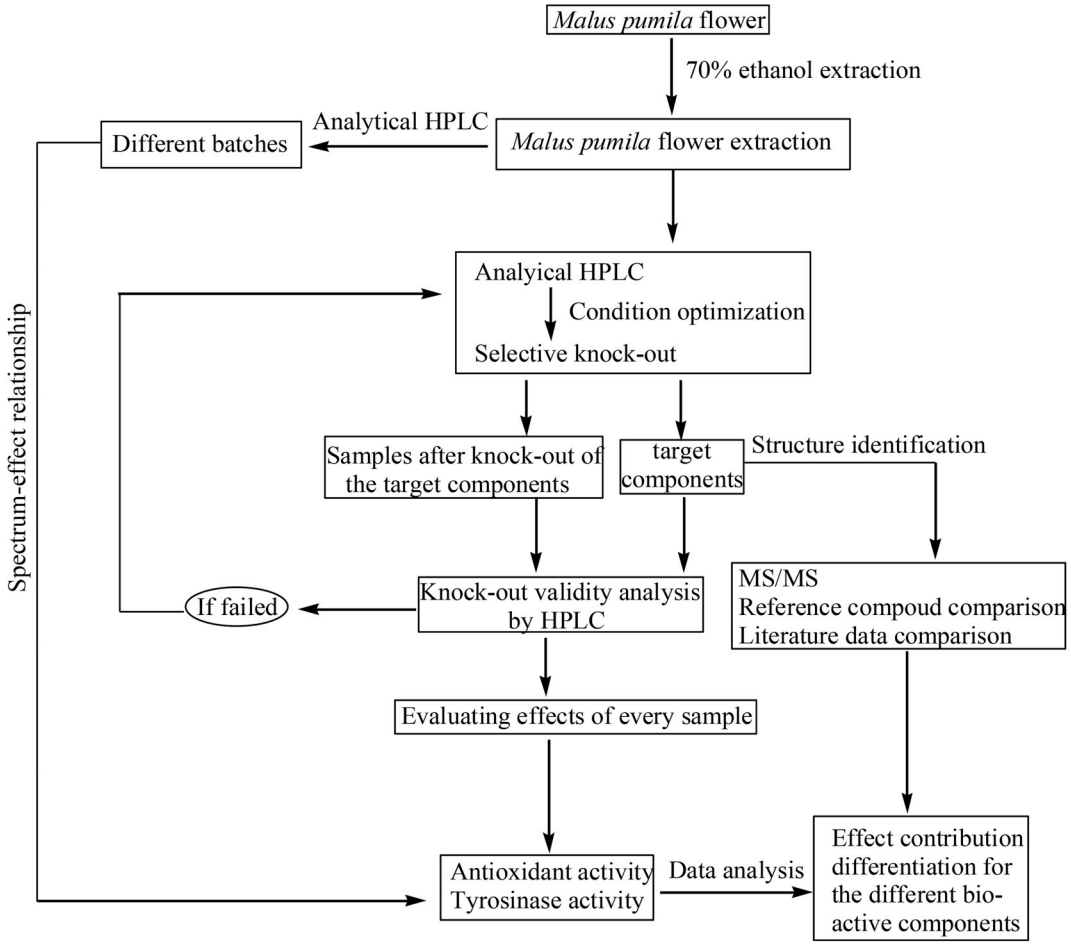

Fig. 1. General flow chart.

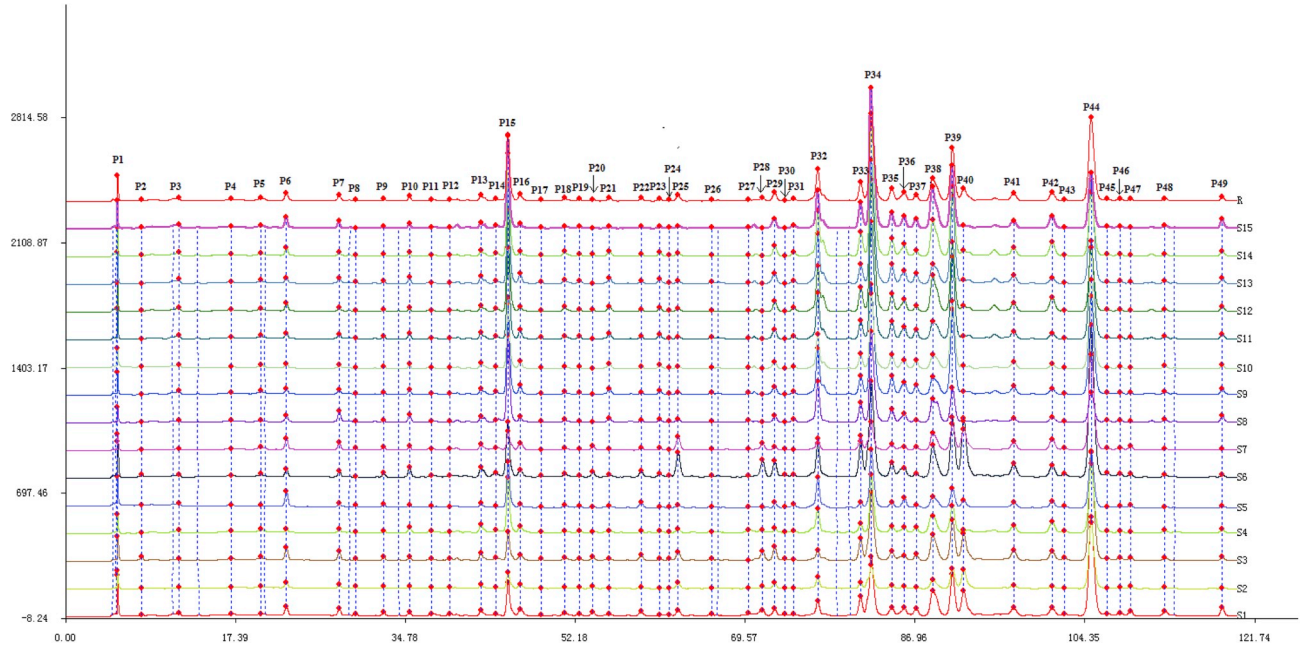

Fig. 2. 15 batches of *M. pumila* flowers HPLC feature peak matching map.

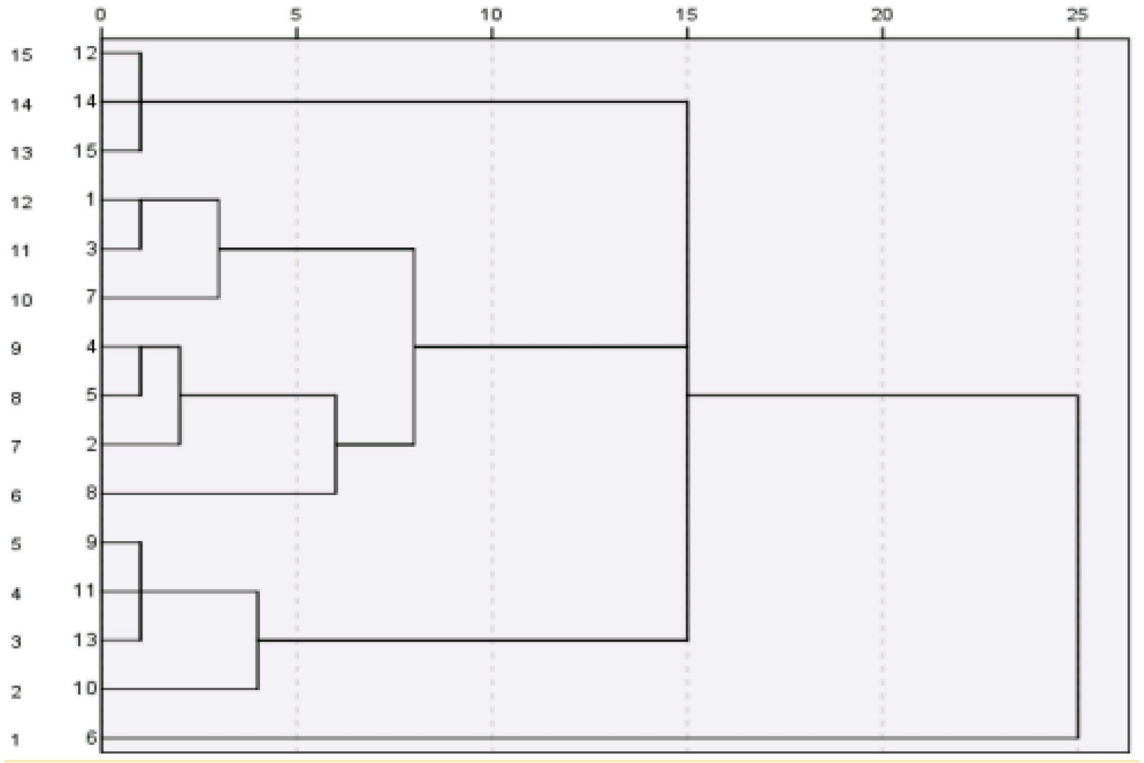

Fig. 3. 15 Cluster Analysis of *M. pumila* flowers.

samples could be grouped into four categories: S12, S14 and S15 belong to one group, S1, S3, S7, S4, S5, S2 and S8 belong to one group, S9, S11, S13 and S10 belong to one group, S6 belongs to one group.

3.1.3. Antioxidant activity of M. pumila flowers in vitro

In Table 3, When the concentration was 1 g/mL (equivalent to the raw material), the antioxidant activity of S1 was the best for the DPPH assay. The antioxidant activity of S2 was the best for ABTS assay.

Table 2
Matching data of characteristic chromatographic peaks in different batches of *M. pumila* flowers by HPLC.

	S1	S2	S3	S4	S5	S6	S7	S8	S9	S10	S11	S12	S13	S14	S15	Contrast fingerprint
S1	1	0.973	0.994	0.95	0.933	0.985	0.968	0.736	0.918	0.94	0.912	0.828	0.912	0.828	0.8	0.953
S2	0.973	1	0.975	0.9	0.885	0.972	0.987	0.626	0.85	0.891	0.84	0.715	0.841	0.715	0.674	0.889
S3	0.994	0.975	1	0.94	0.926	0.988	0.97	0.72	0.905	0.926	0.901	0.816	0.901	0.816	0.79	0.945
S4	0.95	0.9	0.94	1	0.975	0.937	0.901	0.854	0.959	0.968	0.957	0.904	0.958	0.904	0.875	0.977
S5	0.933	0.885	0.926	0.975	1	0.934	0.866	0.883	0.954	0.95	0.958	0.92	0.958	0.92	0.896	0.977
S6	0.985	0.972	0.988	0.937	0.934	1	0.958	0.75	0.909	0.924	0.906	0.828	0.906	0.829	0.8	0.95
S7	0.968	0.987	0.97	0.901	0.866	0.958	1	0.594	0.827	0.875	0.815	0.689	0.816	0.689	0.649	0.871
S8	0.736	0.626	0.72	0.854	0.883	0.75	0.594	1	0.899	0.85	0.91	0.962	0.91	0.962	0.958	0.895
S9	0.918	0.85	0.905	0.959	0.954	0.909	0.827	0.899	1	0.99	0.999	0.952	0.999	0.952	0.927	0.988
S10	0.94	0.891	0.926	0.968	0.95	0.924	0.875	0.85	0.99	1	0.985	0.909	0.985	0.909	0.875	0.98
S11	0.912	0.84	0.901	0.957	0.958	0.906	0.815	0.91	0.999	0.985	1	0.961	1	0.961	0.938	0.989
S12	0.828	0.715	0.816	0.904	0.92	0.828	0.689	0.962	0.952	0.909	0.961	1	0.96	1	0.994	0.953
S13	0.912	0.841	0.901	0.958	0.958	0.906	0.816	0.91	0.999	0.985	1	0.96	1	0.96	0.938	0.989
S14	0.828	0.715	0.816	0.904	0.92	0.829	0.689	0.962	0.952	0.909	0.961	1	0.96	1	0.994	0.953
S15	0.8	0.674	0.79	0.875	0.896	0.8	0.649	0.958	0.927	0.875	0.938	0.994	0.938	0.994	1	0.931
Contrast fingerprint	0.953	0.889	0.945	0.977	0.977	0.95	0.871	0.895	0.988	0.98	0.989	0.953	0.989	0.953	0.931	1

Table 3
Antioxidant Activity of 70% Ethanol Extract from *M. pumila* flowers in Different Batches.

sample	DPPH		ABTS	
	1(g/mL)	IC_{50}(mg/mL)	1(g/mL)	IC_{50}(mg/mL)
S1	91.86	19.71 ± 0.34	78.32	22.20 ± 0.22$^{\#\#\#}$
S2	87.98	36.37 ± 2.18***	97.74	1.93 ± 0.01
S3	92.39	64.20 ± 1.73***	75.16	24.06 ± 0.06$^{\#\#\#}$
S4	89.72	37.17 ± 1.11***	81.18	25.00 ± 0.03$^{\#\#\#}$
S5	82.76	23.53 ± 0.09***	93.87	22.02 ± 0.12$^{\#\#\#}$
S6	90.16	46.73 ± 3.73***	87.61	29.55 ± 0.45$^{\#\#\#}$
S7	99.60	20.30 ± 0.14	80.45	21.37 ± 0.13$^{\#\#\#}$
S8	91.67	28.43 ± 1.13***	80.09	21.31 ± 0.03$^{\#\#\#}$
S9	88.82	33.43 ± 1.33***	83.77	25.24 ± 0.22$^{\#\#\#}$
S10	91.94	18.07 ± 0.10	76.72	26.22 ± 0.34$^{\#\#\#}$
S11	80.59	38.25 ± 2.17***	87.79	9.32 ± 0.09$^{\#\#\#}$
S12	90.66	22.43 ± 0.18**	82.26	4.94 ± 0.09
S13	91.19	34.80 ± 0.61***	87.86	18.51 ± 0.17$^{\#\#\#}$
S14	91.42	30.00 ± 0.60***	85.86	17.48 ± 0.05$^{\#\#\#}$
S15	85.29	30.60 ± 0.21***	85.86	17.33 ± 1.49$^{\#\#\#}$

Note: Compared with S10,$^{*}P < 0.05$,$^{**}P < 0.01$,$^{***}P < 0.001$; Compared with S2, $^{\#}P < 0.05$, $^{\#\#}P < 0.01$, $^{\#\#\#}P < 0.001$.

Table 4
Activation rates of tyrosinase for 70% ethanol extracts from *M. pumila* flowers.

sample	Concentration of Ethanol Extract (Equal to the Amount of Raw Medicinal Herbs)				
	1 g/mL	0.5 g/mL	0.25 g/mL	0.125 g/mL	0.0625 g/mL
S1	293.80 ± 0.01***	155.70 ± 0.08$^{\$\$\$}$	87.15 ± 0.04$^{\&\&\&}$	51.12 ± 0.09$^{\#\#\#}$	21.98 ± 0.36***
S2	198.67 ± 0.04***	−17.27 ± 0.87$^{\$\$\$}$	62.19 ± 0.37$^{\&\&\&}$	−14.88 ± 0.87$^{\#\#\#}$	6.08 ± 0.16***
S3	138.54 ± 0.03***	68.62 ± 0.06$^{\$\$\$}$	41.44 ± 0.05$^{\&\&\&}$	29.94 ± 0.06$^{\#\#\#}$	19.41 ± 0.20***
S4	364.51 ± 0.06	204.58 ± 0.19	84.48 ± 0.35$^{\&\&\&}$	61.41 ± 0.20	38.18 ± 0.27
S5	277.79 ± 0.09***	136.72 ± 0.08$^{\$\$\$}$	69.63 ± 0.43$^{\&\&\&}$	21.55 ± 1.25$^{\#\#\#}$	14.98 ± 0.55***
S6	207.34 ± 0.09***	84.88 ± 0.06$^{\$\$\$}$	48.12 ± 0.07$^{\&\&\&}$	19.29 ± 0.26$^{\#\#\#}$	2.95 ± 0.52***
S7	180.94 ± 0.02***	109.78 ± 0.18$^{\$\$\$}$	47.38 ± 0.07$^{\&\&\&}$	24.07 ± 0.19$^{\#\#\#}$	20.59 ± 0.23***
S8	177.39 ± 0.07***	96.41 ± 0.20$^{\$\$\$}$	33.21 ± 0.70$^{\&\&\&}$	−3.16 ± 2.89$^{\#\#\#}$	−8.02 ± 1.65***
S9	182.58 ± 0.12***	121.12 ± 0.17$^{\$\$\$}$	46.25 ± 0.16$^{\&\&\&}$	6.36 ± 0.48$^{\#\#\#}$	−6.93 ± 0.47***
S10	236.12 ± 0.23***	192.29 ± 0.16	69.12 ± 0.11$^{\&\&\&}$	33.67 ± 0.21$^{\#\#\#}$	8.74 ± 0.49***
S11	283.16 ± 0.08***	162.49 ± 0.23$^{\$\$\$}$	74.05 ± 0.13$^{\&\&\&}$	24.56 ± 0.14$^{\#\#\#}$	2.82 ± 1.20***
S12	222.89 ± 0.04***	145.6 ± 0.17$^{\$\$\$}$	70.98 ± 0.48$^{\&\&\&}$	36.99 ± 0.08$^{\#\#\#}$	4.81 ± 1.65***
S13	242.23 ± 0.02***	150.50 ± 0.25$^{\$\$\$}$	57.61 ± 0.31$^{\&\&\&}$	18.24 ± 2.16$^{\#\#\#}$	0.22 ± 0.71***
S14	222.45 ± 0.04***	229.67 ± 0.05	96.88 ± 0.29	41.22 ± 0.39$^{\#\#\#}$	18.92 ± 0.21***
S15	134.44 ± 0.04***	128.88 ± 0.28$^{\$\$\$}$	71.56 ± 0.26$^{\&\&\&}$	12.10 ± 0.19$^{\#\#\#}$	−1.32 ± 0.18***

Note: Compared with S4 (1 g/mL),$^{*}P < 0.05$,$^{**}P < 0.01$,$^{***}P < 0.001$; compared with S14 (0.5 g/mL),$^{\$}P < 0.05$, $^{\$\$}P < 0.01$, $^{\$\$\$}P < 0.001$; compared with S14 (0.25 g/mL),$^{\&}P < 0.05$, $^{\&\&}P < 0.01$, $^{\&\&\&}P < 0.001$; compared with S4 (0.0625 g/mL),$^{\ast}P < 0.05$, $^{\ast\ast}P < 0.01$,$^{\ast\ast\ast}P < 0.001$.

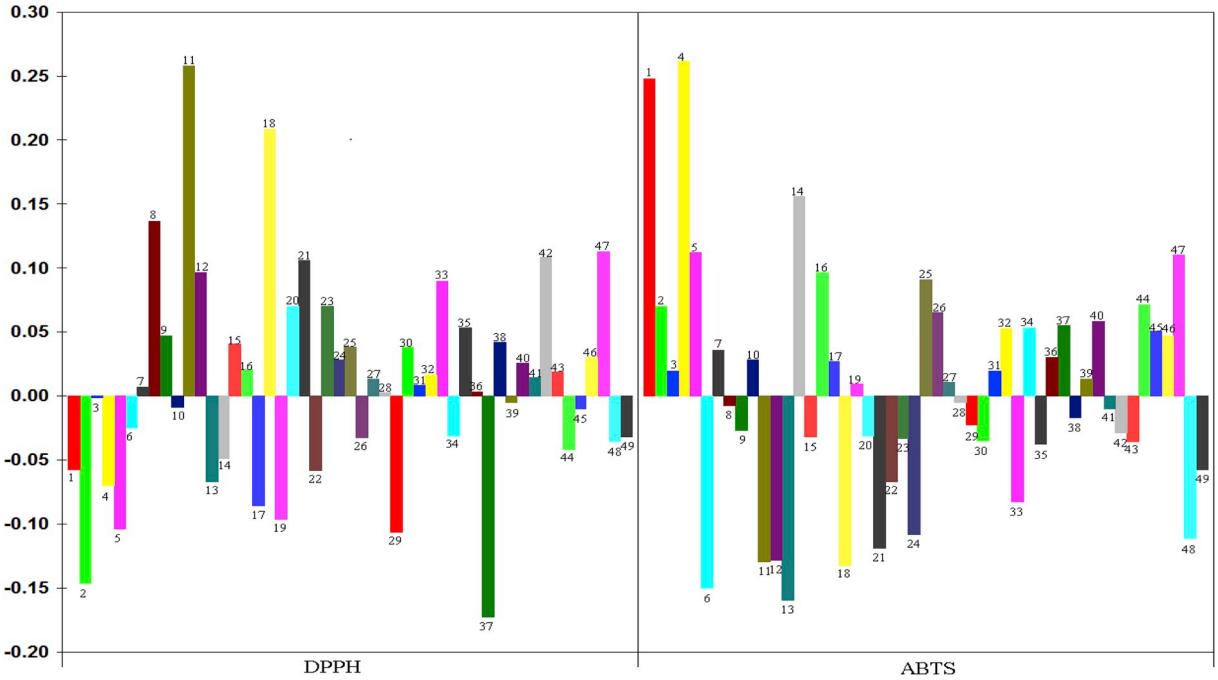

Fig. 4. Standardization regression coefficients of partial least squares analysis (PLSR) equations of *M. pumila* flowers.

3.1.4. Tyrosinase activity of M. pumila flowers in vitro

In Table 4, the ethanol extracts of *M. pumila* flowers had two-way regulation effect on tyrosinase at different concentration. However, when the concentration was 0.5 g/mL and 0.125 g/mL (equivalent to the raw material), the sample S2 showed inhibitory activity of tyrosinase. When the concentration were 0.125 g/mL and 0.0625 g/mL (equivalent to the raw material), the sample S8 showed inhibitory activity of tyrosinase. When the concentration was 0.0625 g/mL (equivalent to the raw material), the samples S9 and S15 showed inhibitory activity of tyrosinase.

In our study, the areas of quantitative chromatographic peaks were set as the independent variable(*X*), activation rate of tyrosinase activity (equivalent to the raw material 1 g/mL) were taken as the dependent variable (*Y*). Then, DPS 7.05 statistical software was used for the mean of the data processing and the partial least squares regression analysis. The results showed that when the potential factor reached 7and 2, R^2 reached maximum and three regression equations were obtained, as follows:

Y1 = 0.000000–0.057517X1-0.146612x2-0.001528X3-0.070310X4-0.103622X5-0.024900X6 + 0.007196X7 + 0.136394X8 + 0.047151X9-0.008886X10 + 0.257668X11 + 0.096412X12–0.066681X13–0.049109X14 + 0.040879X15 + 0.020868X16–0.085546X17 + 0.208471X18–0.096616X19 + 0.070220X20 + 0.105765X21–0.057945X22 + 0.069893X23 + 0.028210X24 + 0.038477X25–0.032349X26 + 0.013085X27 + 0.002519X28–0.106296X29 + 0.038108X30 + 0.008167X31 + 0.015986X32 + 0.089698X33–0.031332X34 + 0.053394X35 + 0.003352X36–0.172745X37 + 0.042004X38–0.004706X39 + 0.025760X40 + 0.014470X41 + 0.108257X42 + 0.018646X43–0.042160X44–0.009990X45 + 0.029840X46 + 0.112787X47–0.035844X48–0.031771X49

Y2 = 0.000000 + 0.247821X1 + 0.069923X2 + 0.019382X3 + 0.261750X4 + 0.111847X5-0.150074X6 + 0.035749X7-0.007461X8-0.027179X9 + 0.028156X10–0.129589X11–0.128238X12–0.159807X13 + 0.155858X14–0.031962X15 + 0.096604X16 + 0.026986X17–0.132730X18 + 0.009233X19–0.031587X20–0.119044X21–0.067034X22–0.033137X23–0.108101X24 + 0.090561X25 + 0.065261X26 + 0.010735X27–0.005237X28–0.022685X29–0.035048X30 + 0.019191X31 + 0.052482x32–0.082500x33 + 0.053517x34–0.037594x35 + 0.030286x36 + 0.055107x37–0.016854x38 + 0.013095-x39 + 0.058344x40–0.009883x41–0.028981x42–0.035819x43 + -0.071179x44 + 0.050623x45 + 0.046987x46 + 0.110448x47–0.111393-x48–0.057823x49

Y3 = 209.178125 + 8.738932X1 + 13.325043X2 + 2.525883X3-2.446275X4 + 0.131851X5-0.569870X6-9.387292X7 + 6.574189X8 + 3.064456X9-1.339687X10–10.421878X11 + 1.911491X12 + 9.421468X13 + 8.051810X14–0.371059X15 + 5.547648X16–2.362022X17 + 2.884962X18–2.797988X19–2.133924X20 + 3.067884X21 + 4.109525X22 + 0.713285X23–15.390761X24–5.304859X25–9.513628X26 + 13.424406X27–2.570192X28–5.698558X29–3.451294X30 + 9.541056X31 + 3.573445X32–10.860261X33–4.440462X34–5.751761X35 + 5.911123X36 + 2.303579X37–2.025045X38–2.474112X39–2.168459X40 + 4.903922X41 + 4.140374X42 + 6.409580X43 + 2.535607X44 + 0.016602X45–1.484484X46 + 4.860115X47 + 6.987505X48–3.511022X49

The regression coefficients of the partial least squares regression equation was in Fig. 4. Chromatographic peaks P8, P11, P18, P21, P42 and P47 were positively correlated with DPPH free radical scavenging capacity, and the correlation coefficient were larger (|R| > 0.1). That is to say, the higher the content of compounds represented by these

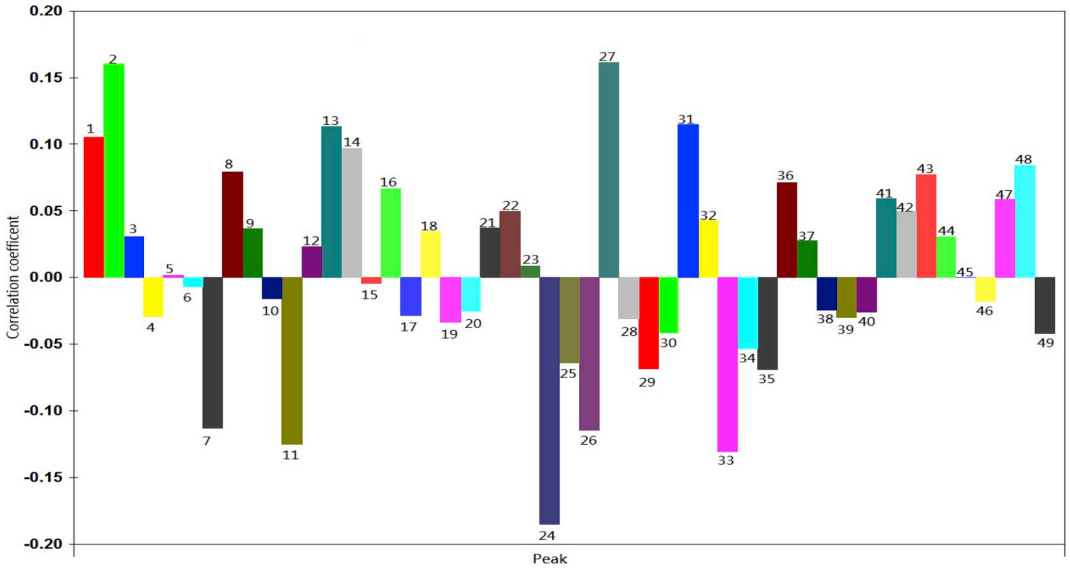

Fig. 5. Standardization regression coefficients of partial least squares analysis (PLSR) equations of *M. pumila* flowers.

peaks, the stronger the DPPH free radical scavenging ability of samples. P2, P5, P29 and P37 were negatively correlated with DPPH free radical scavenging capacity, and the absolute values of correlation coefficients were higher ($|R| > 0.1$). When the content of compounds represented by these peaks increased, the scavenging capacity of DPPH free radicals was weaker.

Chromatographic peaks P1, P4, P5, P14 and P47 were positively correlated with ABTS free radical scavenging capacity and had larger correlation coefficients ($|R| > 0.1$). That is to say, when the content of compounds represented by these peaks increased, the ABTS free radical scavenging capacity of samples were stronger. P6, P11, P12, P13, P18, P21 and P48 were negatively correlated with ABTS free radical scavenging capacity, and the absolute values of correlation coefficients were higher ($|R| > 0.1$). When the content of compounds represented by these peaks increased, the ABTS free radical scavenging capacity of samples was weaker.

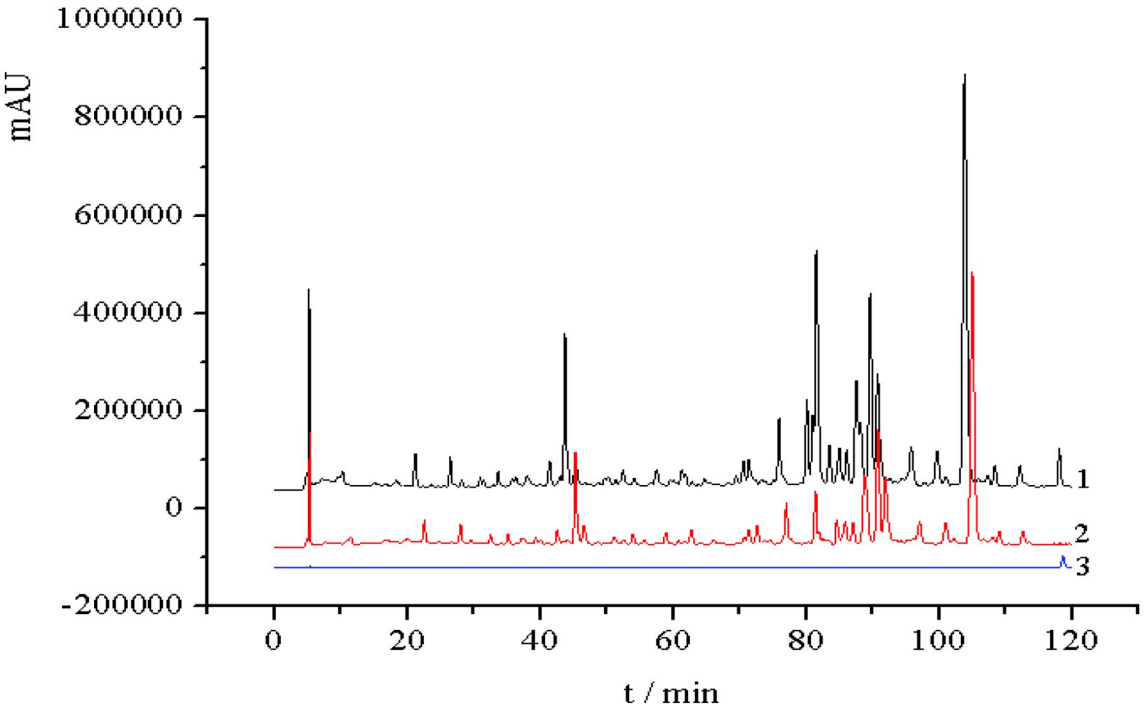

Fig. 6. 1. HPLC of *M. pumila* flowers, 2. HPLC of P49 negative sample, 3. HPLC of target component P49.

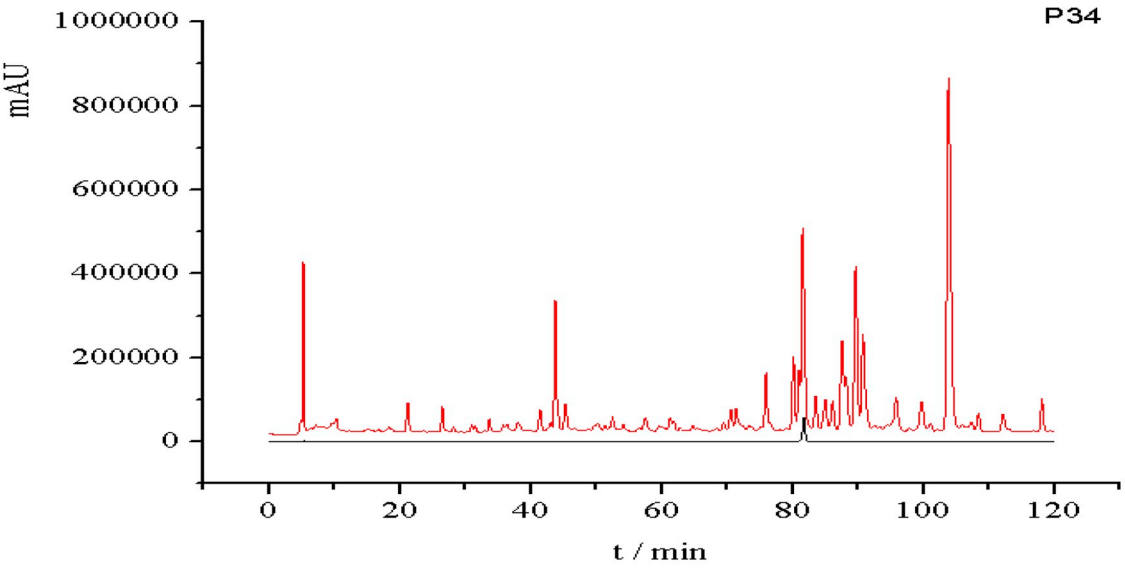

(a)

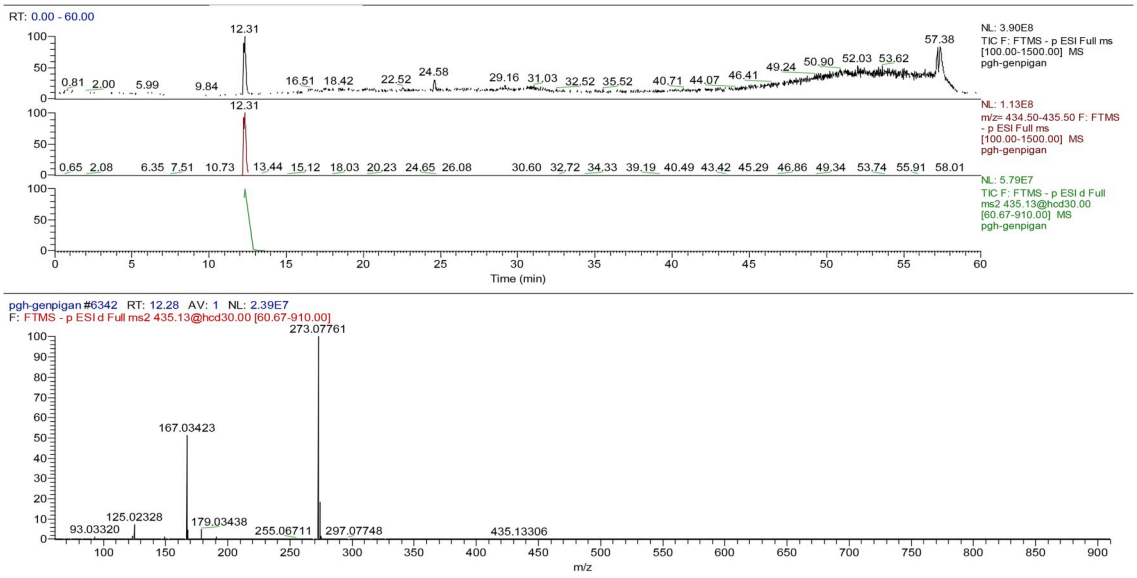

(b)

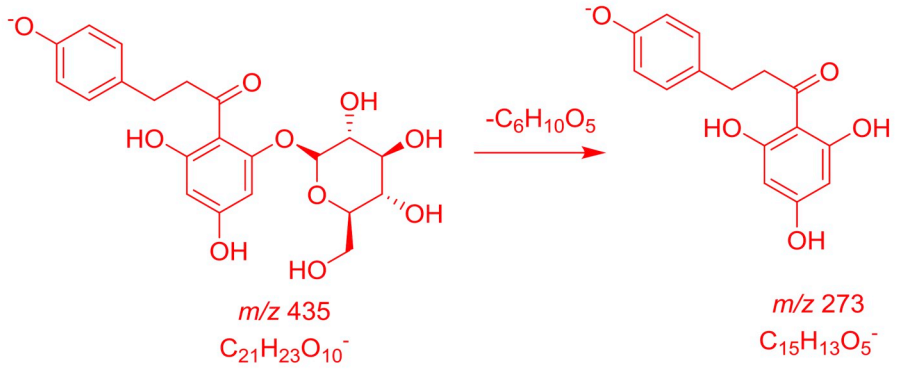

(c)

Fig. 7. (a) HPLC of phloridzin standard and sample, (b) Mass Spectrogram of P34, (c)Fragmentation pathway of P34.

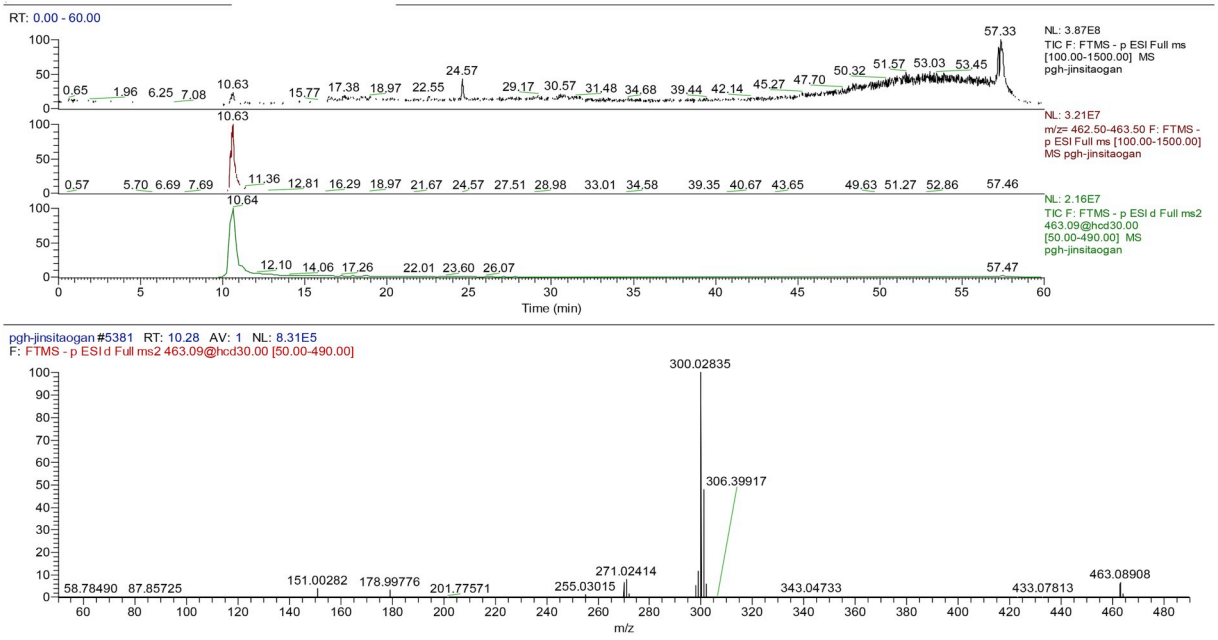

(a)

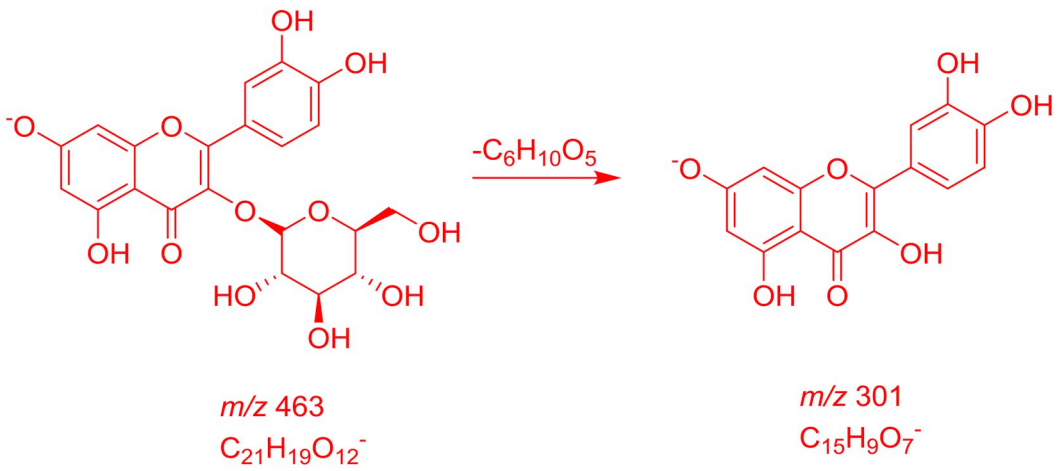

(b)

Fig. 8. (a)Mass Spectrogram of P35, (b)Fragmentation pathway of P35.

The regression coefficients of the partial least squares regression equation was shown in Fig. 5. Chromatographic peaks P1, P2, P13, P14, P27 and P31 were positively related to their activation effects on tyrosinase in *M. pumila* flowers and their correlation coefficients were larger ($|R| > 0.1$), meaning that when the content of compounds represented by these peaks increased, the activity of tyrosinase was stronger. Chromatographic peaks P7, P11, P24, P26 and P33 were negatively related to the activation effects on tyrosinase and the correlation coefficients were larger ($|R| > 0.1$), meaning that when the content of compounds represented by these peaks increased, the activation of tyrosinase activity of samples decreased.

3.2. Component knock-out test

3.2.1. Mass spectrometric analysis of partial knock-out components

The target components were prepared by HPLC, and the remaining negative samples did not contain the target component were shown in Fig. 6. The HPLC of Standard and UPLC-MS/MS diagrams and fragmentation pathways of partially knocked-out components were shown in Figs. 7–12. The results showed that P34, P35, P39, P44, P45 and P49 were phloridzin, hyperoside, astragalin, afzelin, quercetin and kaempferol Yin et al., 2017; Li et al., 2016; Qin, 2016; Sun et al., 2015), respectively. It should be noted that alternative ways of fragmentation that can reasonably interpret the product ions are also possible, the

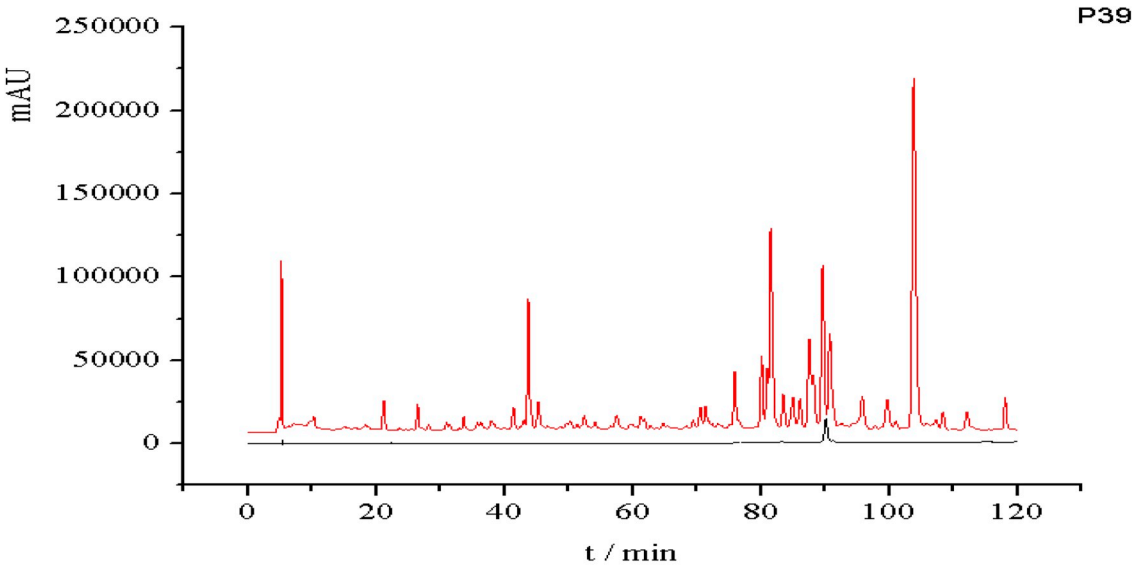

(a)

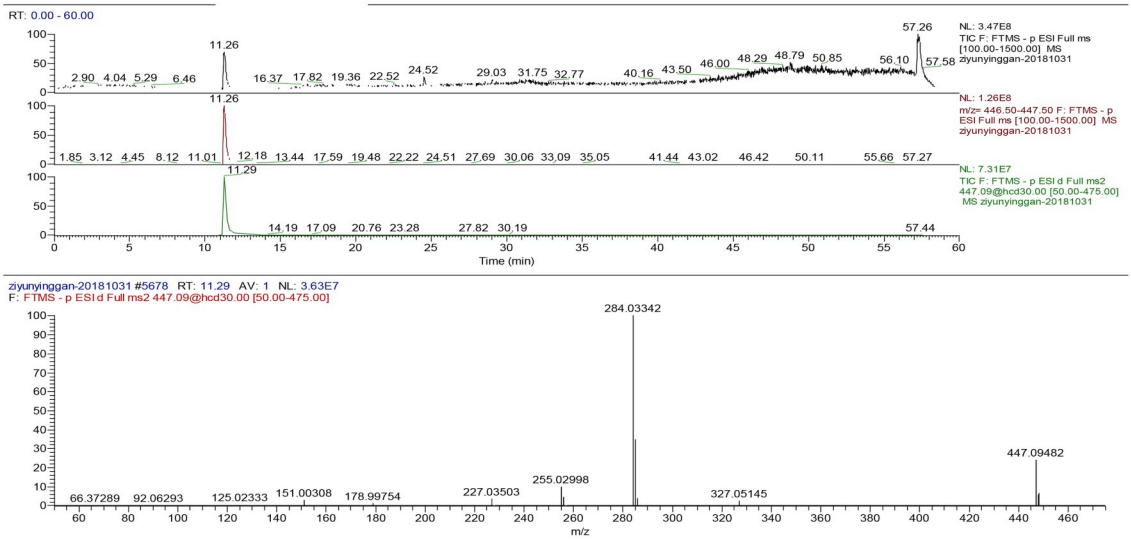

(b)

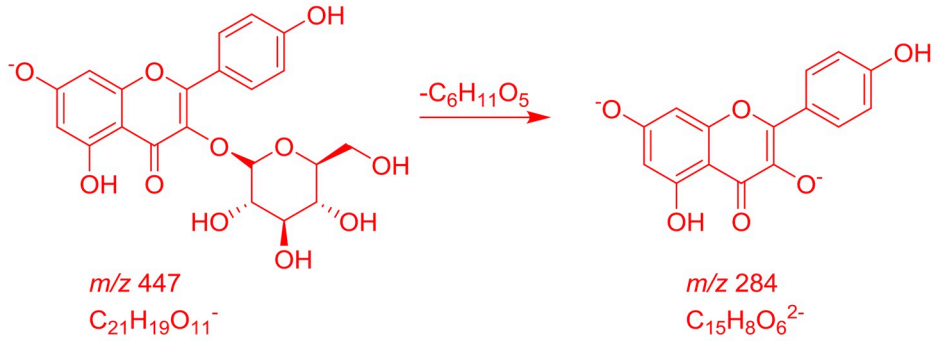

(c)

Fig. 9. (a)HPLC of astragalin standard and sample, (b) Mass Spectrogram of P39, (c)Fragmentation pathway of P39.

(c)Fragmentation pathway of P39

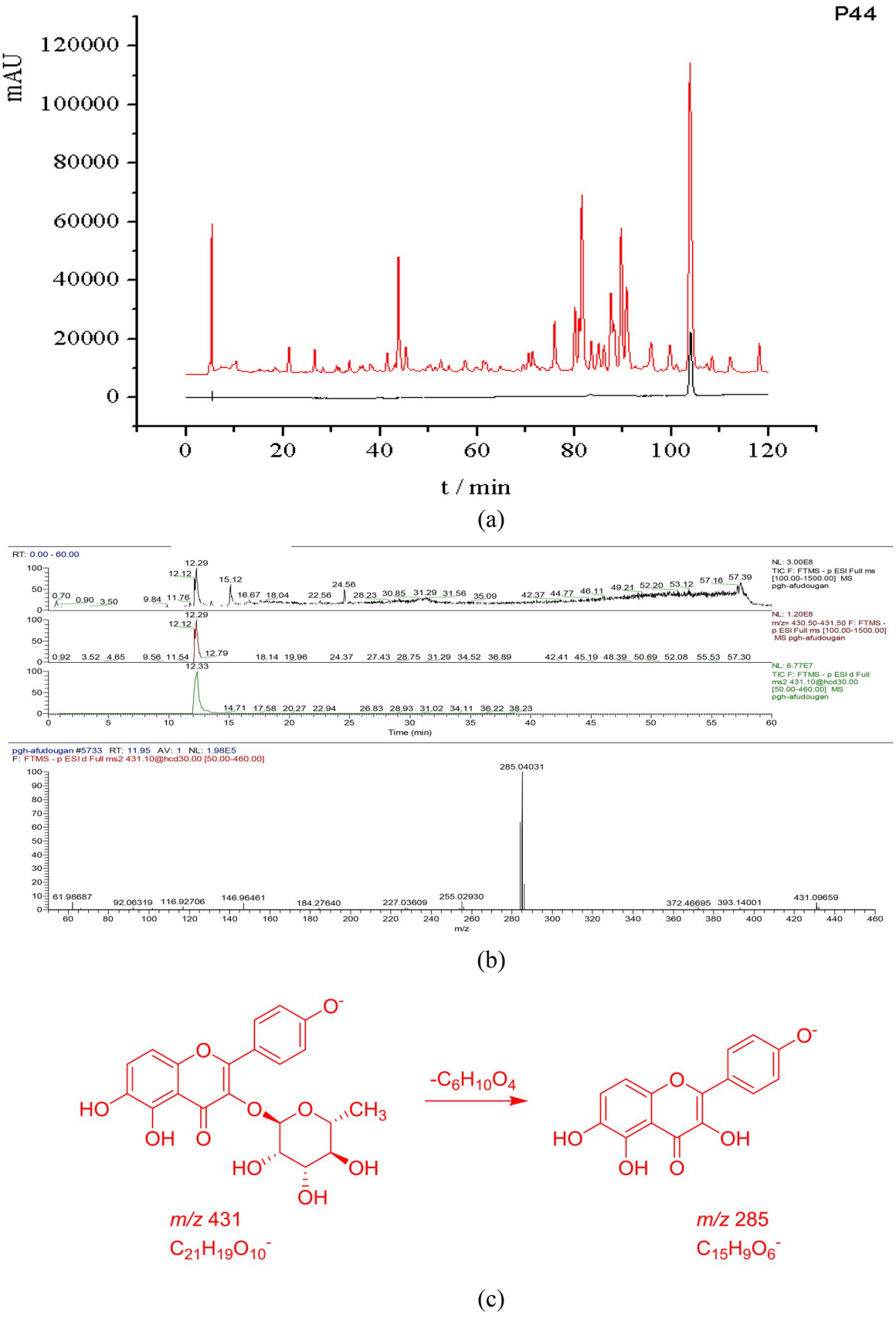

Fig. 10. (a)HPLC of afzelin standard and sample, (b) Mass Spectrogram of P44, (c)Fragmentation pathway of P44.

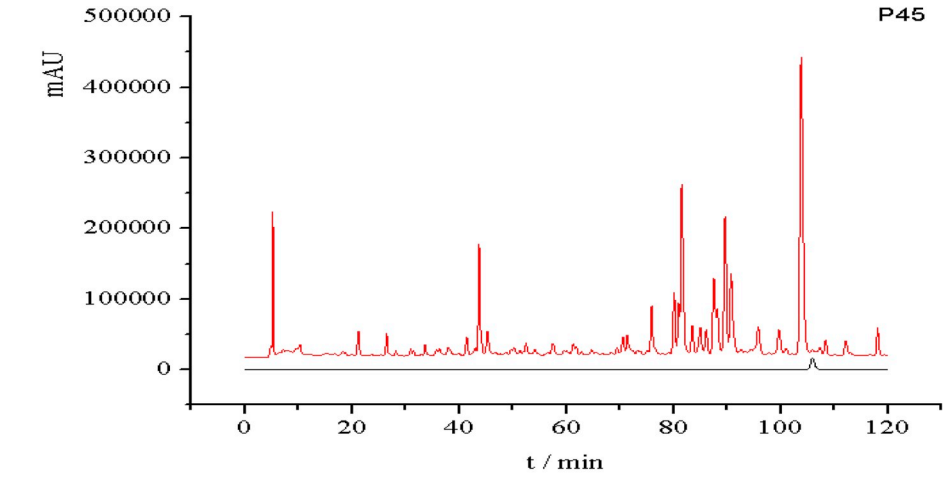

(a)

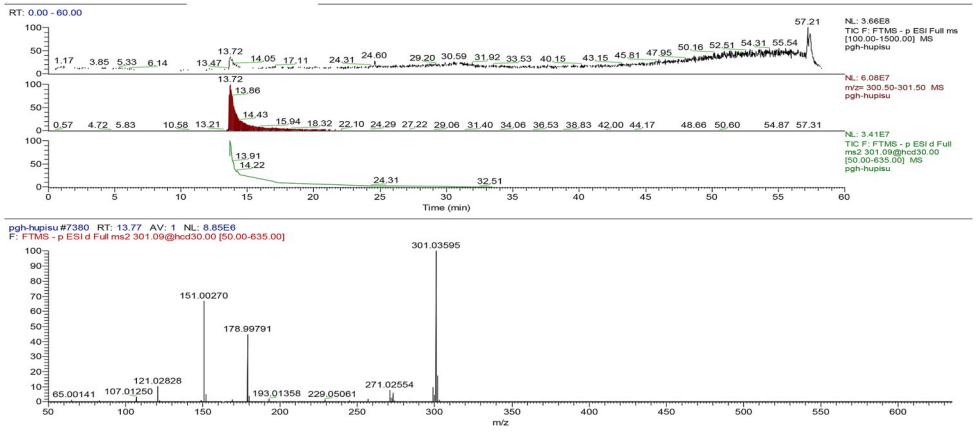

(b)

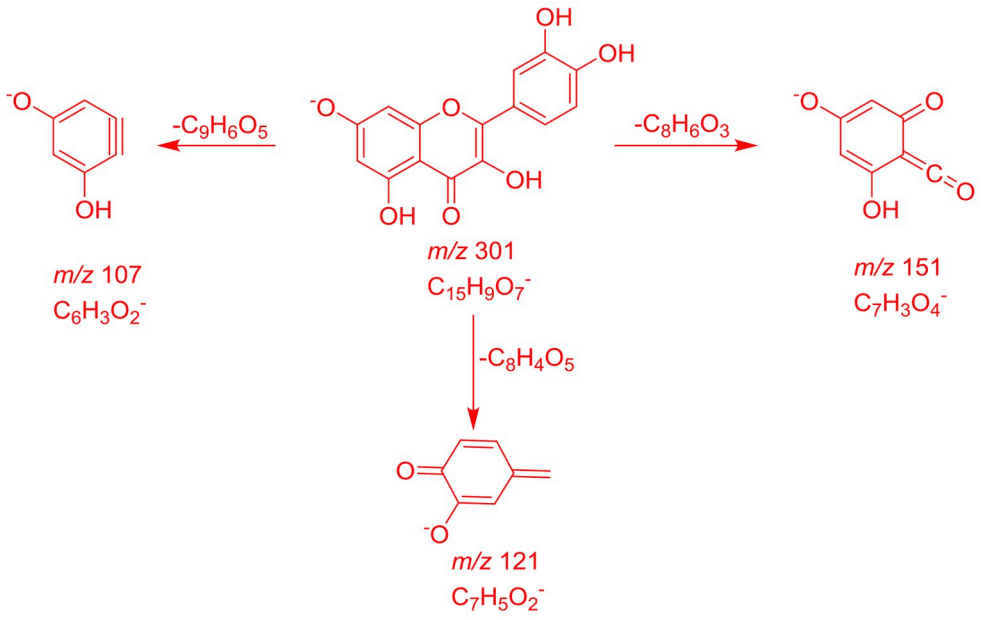

(c)

Fig. 11. (a)HPLC of quercetin standard and sample, (b) Mass Spectrogram of P45, (c)Fragmentation pathway of P45.

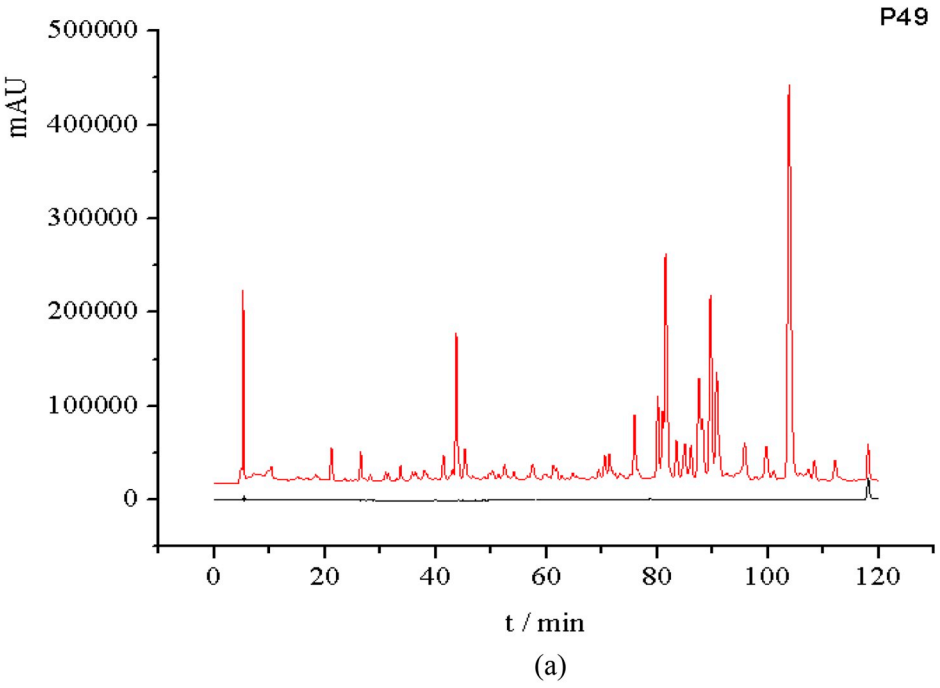

(a)

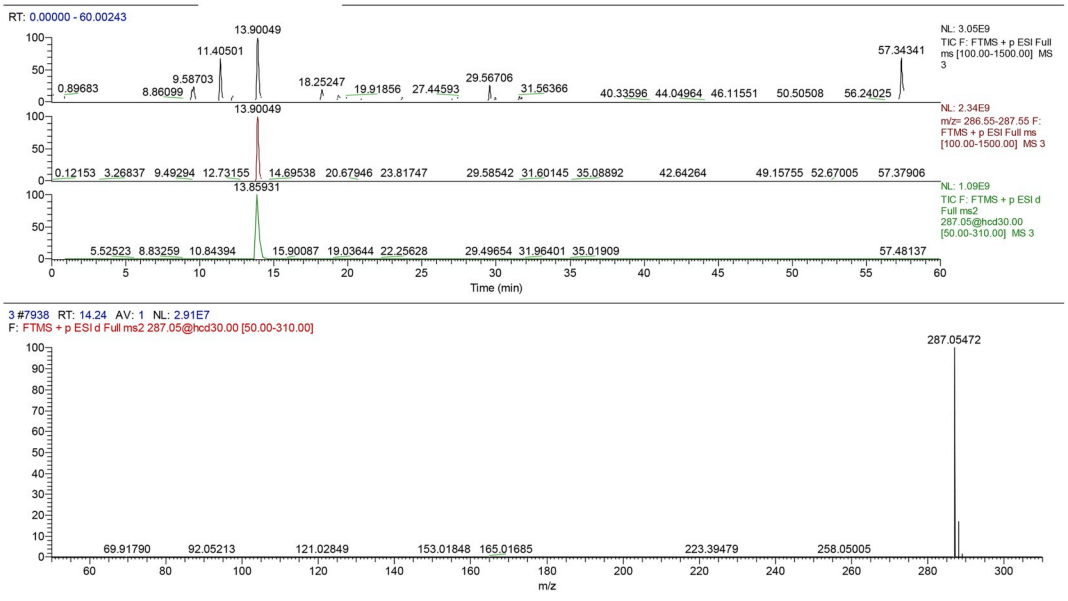

(b)

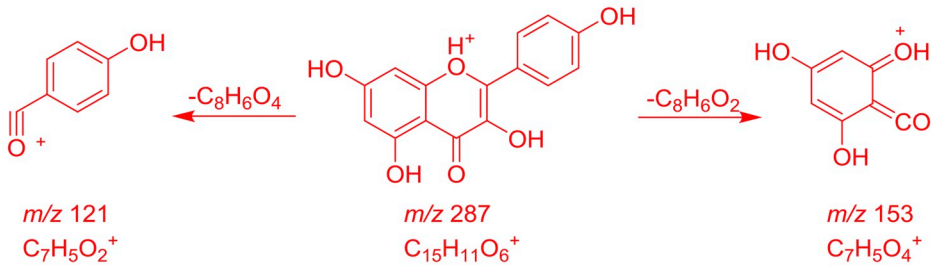

(c)

Fig. 12. (a)HPLC of kaempferol standard and sample, (b) Mass Spectrogram of P49, (c)Fragmentation pathway of P49.

Table 5
Antioxidant activity of knock-out components and negative samples of 70% ethanol extract from *M. pumila* flowers.

Peak	DPPH(%)			ABTS(%)		
	70%Ethanol Extracts	P +	P-	70%Ethanol Extracts	P +	P-
P7	90.72 ± 1.03	–	70.54 ± 1.34	93.31 ± 0.98	11.93 ± 0.66	85.69 ± 0.07
P15	90.72 ± 1.03	18.18 ± 0.38	72.55 ± 0.11	93.31 ± 0.98	61.35 ± 0.01	98.73 ± 0.10
P29	90.72 ± 1.03	15.38 ± 0.04	71.84 ± 0.44	93.31 ± 0.98	60.18 ± 0.09	87.34 ± 1.53
P32	90.72 ± 1.03	15.33 ± 0.12	65.01 ± 2.70	93.31 ± 0.98	57.88 ± 0.02	97.88 ± 1.24
P34	90.72 ± 1.03	–	70.85 ± 4.74	93.31 ± 0.98	22.08 ± 0.04	84.61 ± 1.11
P35	90.72 ± 1.03	45.45 ± 0.57	75.01 ± 2.88	93.31 ± 0.98	–	94.55 ± 2.52
P36	90.72 ± 1.03	9.09 ± 0.01	76.32 ± 1.58	93.31 ± 0.98	51.15 ± 0.29	86.45 ± 1.36
P37	90.72 ± 1.03	6.51 ± .01	64.37 ± 0.56	93.31 ± 0.98	9.98 ± 0.64	88.16 ± 1.38
P38	90.72 ± 1.03	5.85 ± 0.11	84.16 ± 0.10	93.31 ± 0.98	–	90.12 ± 0.46
P39	90.72 ± 1.03	8.77 ± 0.45	77.34 ± 2.12	93.31 ± 0.98	–	78.23 ± 4.02
P40	90.72 ± 1.03	–	93.96 ± 0.28	93.31 ± 0.98	43.63 ± 0.38	95.58 ± 1.47
P41	90.72 ± 1.03	–	91.17 ± 0.40	93.31 ± 0.98	42.24 ± 0.15	96.76 ± 0.98
P42	90.72 ± 1.03	24.20 ± 0.63	82.22 ± 2.72	93.31 ± 0.98	36.57 ± 0.47	98.40 ± 1.27
P44	90.72 ± 1.03	64.89 ± 0.75	89.83 ± 1.09	93.31 ± 0.98	–	96.02 ± 0.93
P45	90.72 ± 1.03	–	77.64 ± 0.33	93.31 ± 0.98	45.48 ± 0.44	98.11 ± 1.42
P48	90.72 ± 1.03	5.50 ± 0.15	64.61 ± 0.76	93.31 ± 0.98	–	99.25 ± 0.72
P49	90.72 ± 1.03	5.87 ± 0.08	75.42 ± 0.84	93.31 ± 0.98	–	99.39 ± 0.68

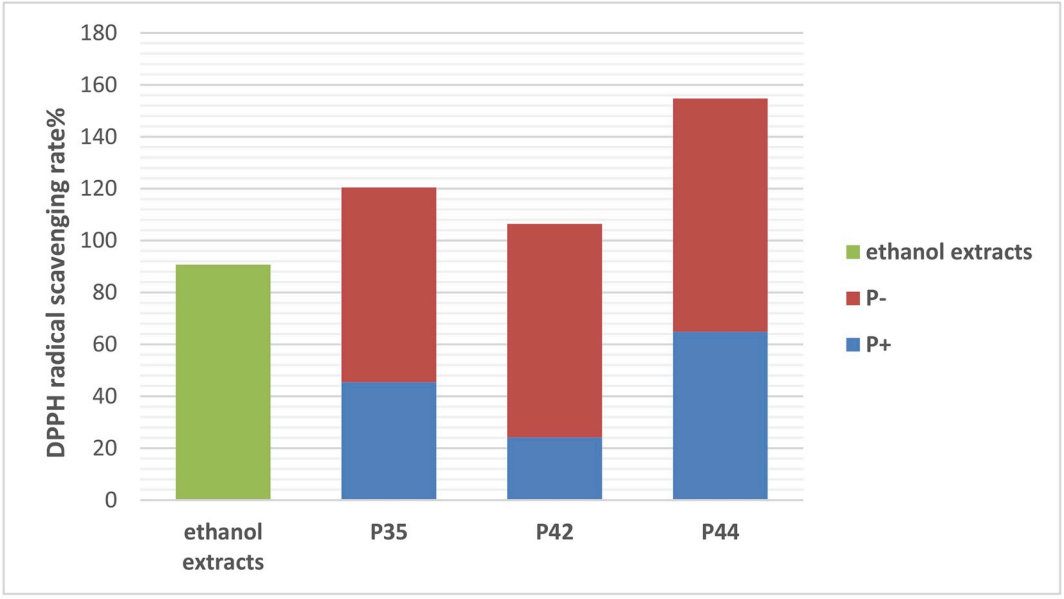

(a) antagonism effect of compounds in *M. pumila* flowers on DPPH

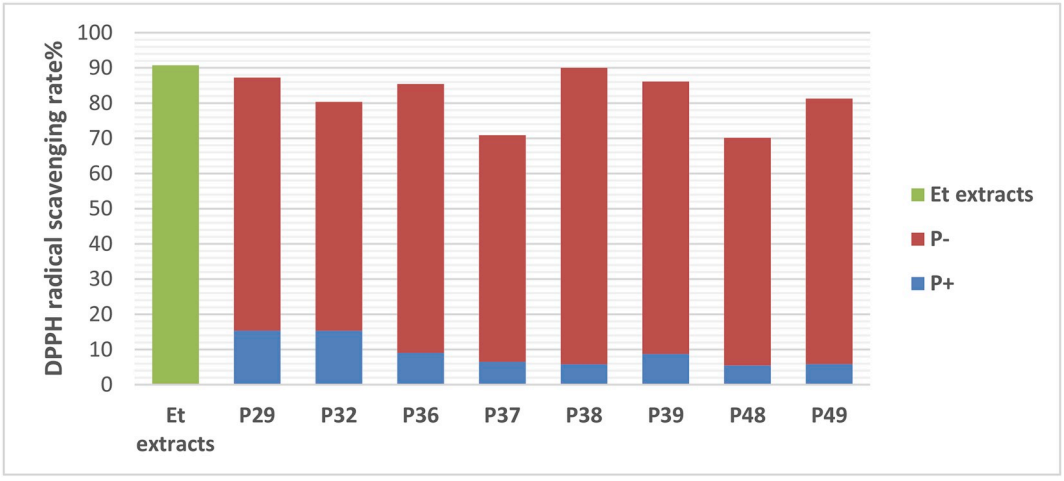

(b) synergistic effect of compounds in *M. pumila* flowers on DPPH

Fig. 13. Antagonism and synergism effect of DPPH free radical scavenging rate.

Table 6
Activation effects of the knocked-out components of water extract of *M. pumila* flowers and negative samples on tyrosinase.

Peak	Activation Rate on Tyrosinase Activity(%)		
	70%Ethanol Extracts	P+	P-
P7	162.19 ± 2.59	−69.49 ± 4.43	−95.71 ± 1.81
P15	162.19 ± 2.59	−19.31 ± 0.97	−100.12 ± 0.34
P29	162.19 ± 2.59	32.15 ± 1.93	−95.24 ± 2.93
P32	162.19 ± 2.59	−3.90 ± 0.04	174.99 ± 0.37
P34	162.19 ± 2.59	−139.32 ± 5.60	−91.74 ± 1.06
P35	162.19 ± 2.59	−6.65 ± 0.23	−98.07 ± 0.42
P36	162.19 ± 2.59	10.85 ± 0.28	95.18 ± 5.06
P37	162.19 ± 2.59	13.81 ± 0.66	96.48 ± 1.46
P38	162.19 ± 2.59	−112.18 ± 2.87	−92.71 ± 1.01
P39	162.19 ± 2.59	8.15 ± 20.19	193.06 ± 3.17
P40	162.19 ± 2.59	21.54 ± 0.52	−116.81 ± 1.73
P41	162.19 ± 2.59	35.17 ± 0.91	135.18 ± 3.35
P42	162.19 ± 2.59	18.10 ± 0.40	−121.29 ± 2.34
P44	162.19 ± 2.59	−13.74 ± 0.09	−123.49 ± 0.53
P45	162.19 ± 2.59	4.36 ± 0.12	98.66 ± 1.34
P48	162.19 ± 2.59	9.79 ± 0.59	−102.54 ± 3.93
P49	162.19 ± 2.59	21.18 ± 0.37	−100.37 ± 3.54

negative charge can be present at any hydroxy group rather than the position denoted.

3.2.2. Knock-out components and negative samples for antioxidant activity

In Table 5, when the concentration of the sample was 1 g/mL (equivalent to the raw material), the components P15, P29, P32, P35, P36, P37, P38, P39, P42, P44, P48 and P49 had the capacity of scavenging DPPH free radicals. Among them, P35, P39, P44 and P49 were identified as hyperoside, astragalin, afzelin and kaempferol by UPLC-MS/MS. It has been reported that antioxidant activity of hyperoside at 0.2 mmol/L was generally more than 3 times higher than that of vitamin E (Ju, 2013). Astragalin, afzelin and kaempferol had the capacity of scavenging DPPH free radicals (Jiao, 2014, Si et al., 2008). The antioxidant activity of these compounds was consistent with that reported in the literatures. Therefore, hyperoside, astragalin, afzelin and kaempferol may be active components in *M. pumila* flowers for scavenging DPPH free radicals.

Except for P35, P38, P39, P44, P48 and P49, the other components had the capacity of scavenging ABTS free radicals, and P7, P32, P34, P36, P37, P40 and P45 were consistent with the results of spectrum-effect relationship analysis. Among them, P34 and P45 were identified as phloridzin and quercetin by UPLC-MS/MS. It has been reported that phloridzin and quercetin were potential antioxidants in *Malus pumila* leaves, *Saccharum officinarum* rinds, and *Coptis chinensis* powders(Lu et al., 2017). The antioxidant activity of phloridzin and quercetin were consistent with that reported in the literatures. So, phloridzin and quercetin may be active components in *M. pumila* flowers for scavenging ABTS free radicals.

In Fig. 13 (a), the total DPPH free radical scavenging rates of P35, P42 and P44 and their negative samples were higher than those of ethanol extracts. It suggested that there might be antagonism effect between the target components and negative samples.

In Fig. 13 (b), the total DPPH free radical scavenging rates of P29, P32, P36, P37, P38, P39, P48 and P49 and their negative samples were lower than those of ethanol extracts. It indicated that there might be synergistic effect between the target components and negative samples.

Except for P35, P38, P39, P44, P48 and P49, the total ABTS free radical scavenging rates of other target components and their negative samples were higher than those of ethanol extracts. It suggested that there might be antagonism effect between the target components and their negative samples on ABTS free radical scavenging.

3.2.3. Knock-out components and negative samples on tyrosinase activity

In Table 6, when the concentration of the sample was 1 g/mL (equivalent to the raw material), P29, P32, P36, P37, P39 (astragalin), P40, P41, P42, P45 (quercetin), P48 and P49 (kaempferol) had activation effects on tyrosinase, among which P41 had the strongest activation effect on tyrosinase. Nagata (Nagata et al., 2010) found that quercetin stimulates melano genesis by increasing tyrosinase activity and decreasing other factors such as melanogenic inhibitors. In our previous studies, we found that astragalin could activate tyrosinase. The activity of astragalin and quercetin were consistent with previous studies. So, astragalin and quercetin and kaempferol were active components in *M. pumila* flowers for the activition of tyrosinase. Howere, it has been reported that kaempferol could inhibit tyrosinase activity (Zhang et al., 2017; Solimine et al., 2016). But, kaempferol could activate tyrosinase in *M. pumila* flowers, This may be the different activity of tyrosinase at different concentrations, or the different mechanism of action.

The P7, P15, P34 (phloridzin), P35 (hyperoside), P38 and P44 (afzelin) had inhibitory effects on tyrosinase, and P34 and P38 had stronger inhibitory effects on tyrosinase. Except for P29, P39 and P49, the other target components were consistent with the results of spectrum-effect relationship analysis. Ziaullah et al. (Bhullar et al., 2013) found that phloridzin could inhibit tyrosinase activity. Some studies had shown that hyperoside and afzelin could interfere melanin production by inhibiting tyrosinase activity (Yin et al., 2016; La, 2011). The inhibition rate of hyperoside on tyrosinase reached more than 50% (Zhang et al., 2011). The tyrosinase activity of these compounds were consistent with that reported in the literatures. We preliminarily speculated that phloridzin, hyperoside and afzelin had strong antagonism effects with other components. The *M. pumila* flowers maybe have activate tyrosinase because of them.

In Fig. 14 (a), the target components of P32, P39 and P41 and their negative samples had an activation effect on tyrosinase, which were consistent with the action direction of total ethanol extracts. The tyrosinase activation rates of these target components and negative samples were higher than that of total ethanol extracts. This indicated that there might be antagonism effect between target components and negative samples on tyrosinase activation.

In Fig. 14 (b), the target components of P7, P34 and P38 and the negative samples had inhibitory effect on tyrosinase, which were contrary to the action direction of total ethanol extracts. It indicated that there might be antagonism effect between target components and negative samples on tyrosinase activation.

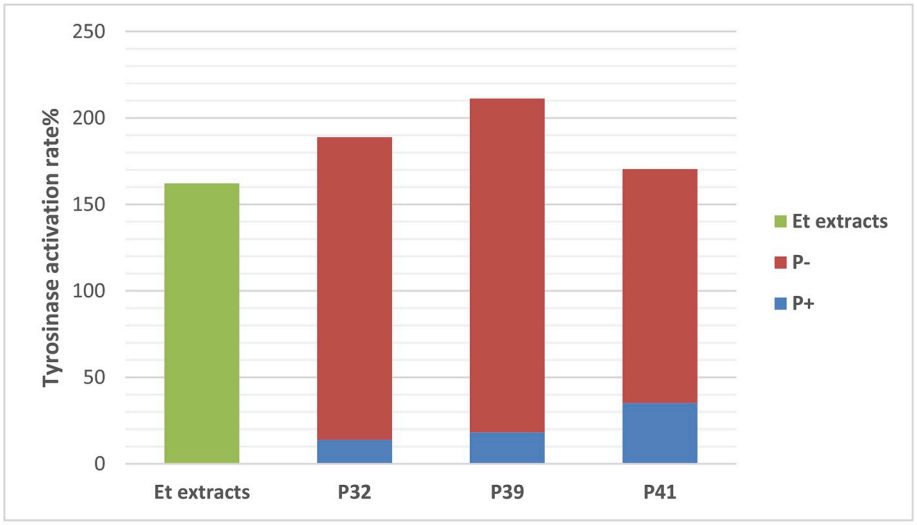

(a)

(b)

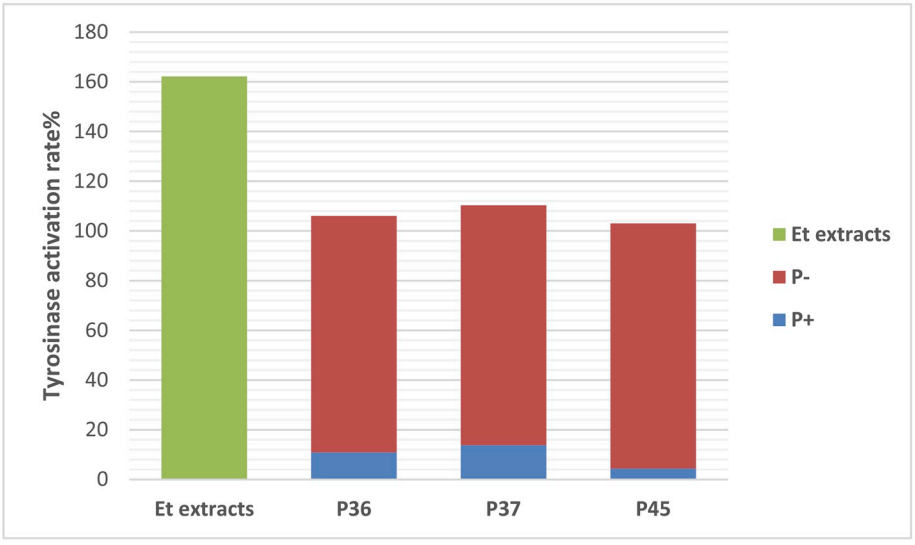

(c)

Fig. 14. Effect between knocked-out components and negative samples of *M. pumila* flowers: (a) Antagonistic effect on tyrosinase inhibition effect; (b) Antagonistic effect on tyrosinase inhibition effect; (c)) Synergetic effect.

In Fig. 14 (c), the target components of P36, P37 and P45 and their negative samples had activation effects on tyrosinase, which were consistent with the action direction of total ethanol extracts. The tyrosinase activation rates of these target components and negative samples were lower than those of total ethanol extracts. It indicated that there might be synergistic effect between target components and negative samples on tyrosinase activation (Peng, 2017).

4. Conclusion

17 knockout components and their negative samples were prepared by HPLC. Six compounds were identified by UPLC-MS/MS. Chromatographic peaks P34, P35, P39, P44, P45 and P49 were phloridzin, hyperoside, astragalin, afzelin, quercetin and kaempferol. Hyperoside and kaempferol were discovered in *M. pumila* flowers for the first by UPLC-MS/MS. The activity of antioxidant and tyrosinase of six compounds in *M. pumila* flowers were proved. P35 was consistent with the spectrum-effect relationship on DPPH free radical scavenging capacity. P34 and P45 were consistent with the spectrum-effect relationship on ABTS free radical scavenging capacity. P45 were consistent with the spectrum-effect relationship on tyrosinase activation. P34 and P35 were consistent with the spectrum-effect relationship on inhibition of tyrosinase.

Abbreviations

M pumila flowers: *Malus pumila* flowers; HPLC: high-performance liquid chromatography; RSD: relative standard deviation; DPPH: 1,1-diphenyl-2-picrylhydrazyl; ABTS: 2.2-Azinobis(3-ethylbenzo-thiazoline-6-sulfoncicacid); BHT: Butylatedhydroxytoluene; BHA: butyl-phydroxyanisole; PG: propyl gallic acid; TCM: Traditional Chinese Medicine.

Author contributions

Wenyi Kang and Zhenhua Liu conceived the research idea. Wenjing Li, Yan Zhang, Shujin Shi and Gen Yang collected the plant specimens, conducted the experiments, analyzed and interpreted the data as well as prepared the first draft. Wenyi Kang, Jinmei Wang and Zhenhua Liu critically read and revised the paper. All authors read and approved the final manuscript.

Competing interests

The authors declare that they have no competing interests.

Funding

This work was supported by Key Project in Science and Technology Agency of Henan Province (182102110473), Innovation and Entrepreneurship Training Program, Henan University (201810475069).

Acknowledgments

We thank other workers in Hebei Food Inspection and Research Institute for the help in MS analysis.

Transparency document

Transparency document related to this article can be found online at https://doi.org/10.1016/j.fct.2019.110754.

References

Bhullar, K.S., Warnakulasuriya, S.N.,, Rupasinghe, H.P.V., 2013. Biocatalytic synthesis, structural elucidation, antioxidant capacity and tyrosinase inhibition activity of long chain fatty acid acylated derivatives of phloridzin and isoquercitrin. Bioorg. Med. Chem. 21, 684–692.

Cai, L., Zhang, Q., Yang, F.Q., 2017. Applications progress on spectrum-effect relationship in study of Chinese materia medica. Chin. Tradit. Herb. Drugs 48, 5005–5011.

Cui, F., Han, Z.H., Liu, X.H., et al., 2016. Spectrum-effect relationship of active fraction from Hedysari Radix on improving immunity. Chin. Tradit. Herb. Drugs.

1974. Flora of China Beijing: Science Press .

Gong, G.W., Li, N., Lau, K.M., et al., 2015. Calycosin orchestrates the functions of Danggui Buxue Tang, a Chinese herbal decoction composing of *Astragali Radix* and *Angelica Sinensis* Radix: an evaluation by using calycosin-knock out herbal extract. J. Ethnopharmacol. 168, 150–157.

Jiao, S.M., 2014. Study on extraction of astragalin from hamamelis mollis by ultrasonic-assisted extraction and antioxidation. The Food Industry 35, 51–53.

Ju, M., 2013. Tudies on the Antioxidant Activity and Synergistic Effects of Three Natural Antioxidants. Nanjing Normal University.

Kang, W.Y., Li, C.F., Liu, Y.X., 2010. Antioxidant phenolic compounds and flavonoids of Mitragyna rotundifolia (Roxb.) Kuntze *in vitro*. Med. Chem. Res. 19, 1222–1232.

Kang, W.Y., Song, Y.L., Zhang, L., 2011. α - glucosidase inhibitory and antioxidant properties and antidiabetic activity of Hypericum ascyron L. Med. Chem. Res. 20, 809–816.

La, X.Q., 2011. Chemical Constituents and Bioactivities from Twigs of Myricaria Germanica, a Tibetian Medicine. Qinghai Normal University.

Li, W., Feng, Y.L., Lin, T.E., et al., 2016. Rapid analysis on flavonoids in glechoma longituba(Nakai)Kupr by UPLC-Q-TOF/MS couple with diagnostic ions. J. Chin. Mass Spectrom. Soc. 37, 504–516.

Li, W.J., Shi, M.J., Wang, P.Y., et al., 2018. Efficient determination of three flavonoids in *Malus pumila* flowers by ionic liquid-HPLC. J. Mol. Liq. 8, 139–146.

Liu, X., Huang, C.Y., Yang, Y.F., et al., 2016. HPLC Fingerprint of Dan'e Fukang Decocted Extract Based on Hierarchical Clus. Chin. J. Pharm. 47, 1388–1393.

Lu, Y.Z., Wu, N., Fang, Y.T., et al., 2017. An automatic on-line 2,2-diphenyl-1-picrylhydrazyl-high performance liquid chromatography method for high-throughput screening of antioxidants from natural products. J. Chromatogr. A 1521, 100–109.

Nagata, H., Takekoshi, S., Takeyama, R., et al., 2010. Quercetin enhances melanogenesis by increasing the activity and synthesis of tyrosinase in human melanoma cells and in normal human melanocytes. Pigment Cell Res. 17, 66–73.

Peng, L.N., 2017. Study on the Relevance of Angelica Dahurica Radix and Tyrosinase Activity.

Qin, X., 2016. Identification, Metabolism and Bioactivity Analysis of the Flavonoids in Malus Crabapple Plants.

Shi, M.J., Zhang, Y., Song, M.M., et al., 2018. Screening the marker components in *Psoralea corylifolia* L. With the aids of spectrum-effect relationship and component knock-out by UPLC-MS^2. Int. J. Mol. Sci. 19, 3439.

Si, C.L., Liu, Z., Hui, L.f., et al., 2008. Chemical constituents and antioxidant activities of the extractives from Juglansm and shurica maxim. Bar. Chem. Ind. Fore. Prod. 28, 29–32.

Solimine, J., Garo, E., Wedler, J., et al., 2016. Tyrosinase inhibitory constituents from a polyphenol enriched fraction of rose oil distillation wastewater. Fitoterapia 108, 13–19.

Sun, D.M., Dong, Y.J., Xu, A.L., et al., 2015. Rapid analysis on flavonoids in gegen Zhiju soft capsule by UPLC/Q-TOF-MS. Chin. Tradit. Herb. Drugs 46, 970–976.

Wang, Y.L., Tang, Y.P., Liu, X., et al., 2014. Study on material base of Carthamus tinctorius with antioxidant effect based on selective knock-out. China J. Chin. Mater. Med. 39, 1285–1289.

Wang, J.M., Yao, C., Li, C.Q., et al., 2017a. Spectrum-effect relation of antioxidant activity of flos carthami based on DPPH, ABTS and FRAP assay. Chin. Pharmaceut. J. 825–831.

Wang, J.M., Peng, L.N., Shi, M.J., et al., 2017b. Spectrum effect relationship and component knock-out in angelica dahurica radix by high performance liquid chromatography-Q exactive hybrid quadrupole-orbitrap Mass spectrometer. Molecules 22, 1231.

Xiao, S., 2013. A Method for Research of Antibacterial Constituent Recognition of Traditional Chinese Medicine (Acalypha Australis Linn.) by Spectrum-Effect Relationship.

Xiao, X.H., Yan, D., Yuan, H.L., et al., 2009. Novel patterns of efficient components recognition and quality control for Chinese materia medica based on constituent knock-out/knock-in. Chin. Tradit. Herb. Drugs 40, 1345.

Xu, J.J., 2014. Studies in Quality Control and Evaluation Method of Menthae Haplocalycis Herba Based on the Correlation between its Chromatographic Fingerprint and Antioxidant Activity.

Xu, G.L., Xie, M., Yang, X.Y., et al., 2014. Spectrum-effect relationships as a systematic approach to traditional Chinese medicine research: current status and future perspectives. Molecules 19, 17897–17925.

Yin, Y.Z., Li, Y.W., Han, H.Q., et al., 2016. HPLC fingerprint of pumila flos. Central South Pharmacy 14, 684–687.

Yin, Z.H., Sun, C.H., Fang, H.Z., et al., 2017. Analysis and comparison on fragmentation behavior of quercetin and morin by ESI-MS. J. Instrum. Anal. 36, 205–211.

Yin, Z.H., Zhang, Y., Zhang, J.J., et al., 2018. Coagulatory active constituents of *Malus pumila. Mill.* fowers. Chem. Cent. J. 12, 126.

Zeng, L.J., Lin, B., Song, H.T., 2015. Progress in study of spectrum -effect relationship of traditional Chinese medicine and discussions. China J. Chin. Mater. Med. 40, 1425–1432.

Zhang, T., Pu, Y., Zhao, P., et al., 2011. The detection of component and activity scanning from common medicinal plants in changbai mountain area. Journal of Yanbian University 37, 165–170.

Zhang, L., Yan, J., Liu, X., et al., 2012. Pharmacovigilance practice and risk control of Traditional Chinese Medicine drugs in China: current status and future perspective. J.

Ethnopharmacol. 140, 519–525.
Zhang, W., Yin, Z.H., Peng, T., et al., 2014. Effect of high-temperature heat treatment of Psoralea corylifolia on the activity of tyrosinase. Chin. J. Exp. Tradit. Med. Formulae 20, 71–73.
Zhang, L.Z., Xu, J., Shu, Q.L., et al., 2017. The antioxidant and antityrosinase activities of carvacrol. Mod. Food Sci. Technology. 33, 84–88.
Zhao, X.P., Fan, X.H., Xu, J., et al., 2004. A method for predicting activity of traditional Chinese medi cine based on quantitative composition-activity relationship of neural network model. China J. Chin. Mater. Med. 29, 1082.
Zhao, X.M., Pu, S.B., Zhao, Q.G., et al., 2016. Preliminary study on effective components of Tripterygium wilfordii for liver toxicity based on spectrum-effect correlation analysis. China J. Chin. Mater. Med. 41, 2915–2921.
Zheng, Q., Zhao, Y., Wang, J., et al., 2014. Spectrum-effect relationships between UPLC fingerprints and bioactivities of crude secondary roots of Aconitum carmichaelii Debeaux (Fuzi) and its three processed products on mitochondrial growth coupled with canonical correlation analysis. J. Ethnopharmacol. 153, 615–623.
Zhou, J.L., Qi, L.D., Li, P., 2008. Quality control of Chinese herbal medicines with chromatographic fingerprints. Chin. J. Chromatogr. 26, 153–159.